Wind and Structures, Vol. 12, No. 3 (2009) 259-279
DOI: http://dx.doi.org/10.12989/was.2009.12.3.259

Some aspects of the dynamic cross-wind response of tall industrial chimney

Piotr Górski*

Opole University of Technology, ul. Katowicka 48, Opole, Poland

(Received July 30, 2008, Accepted March 26, 2009)

Abstract. The paper is concerned with the numerical study of the cross-wind response of the 295 m-tall six-flue industrial chimney, located in the power station of Belchatow, Poland. The response of the chimney due to turbulent wind flow is caused by the lateral turbulence component and vortex excitation with taking into account motion-induced wind forces. The cross-wind response has been estimated by means of the random vibration approach. Three power spectral density functions suggested by Kaimal, Tieleman and Solari for the evaluation of the lateral turbulence component response are taken into account. The vortex excitation response has been calculated by means of the Vickery and Basu's model including some complements. Motion-induced wind forces acting on a vibrating chimney have been modeled as a nonlinear aerodynamic damping force. The influence of three components mentioned above on the total cross-wind response of the chimney has been investigated. Moreover, the influence of damping ratios, evaluated by Multi-mode Random Decrement Technique, and number of mode shapes of the chimney have been examined. Computer programmes have been developed to obtain responses of the chimney. The numerical results and their comparison are presented.

Keywords: numerical analysis; tall chimney; lateral and vortex shedding responses; motion-induced wind force.

1. Introduction

In case of a turbulent wind flow around a tall slender structure with circular cross-section, like chimneys, TV-towers, tubes, etc., a complete analysis of the dynamic cross-wind response of such structures requires that the lateral turbulence component response, vortex excitation response and motion-induced response are evaluated.

Among all components mentioned above the vortex excitation acting on slender structures is most important phenomena, although during recent decades is one of the most controversial topic of the wind engineering. The correct prediction of the vortex-induced vibration amplitude is rather complicated. There are two classes of calculation models for vortex shedding response of slender structures: (a) those based on sinusoidal excitation and (b) those based on random excitation.

A sinusoidal excitation model, for vortex shedding response prediction, was developed by Ruscheweyh, *et al.* (1982, 1996, 1998) - presented in the Eurocode Standard (Approach 1, 2003),

* Corresponding Author, E-mail: p.gorski@po.opole.pl

and also by Flaga (1996, 1997). Such models are rather adequate for calculation of the vortex shedding response of structures for which the Scruton number is small (steel chimneys, bridge hangers, antena masts, etc.). In this case the response becomes sinusoidal.

A random excitation model, for vortex shedding and lateral turbulence component response prediction, was developed by Vickery and Basu (1983, 1994, 1995). In this model the lift forces caused by vortex shedding are described by four aerodynamic parameters. These parameters were calibrated from full-scale measurements of tall concrete chimneys (Vickery and Basu 1983, Sanada, *et al.* 1992, Waldeck 1992). So, this model is specially applicable to these types of structures for which the Scruton number is greater (tall industrial chimneys, TV-towers) and for which the response becomes random. Such rightness is confirmed based on a comparative study of some models existing in literature presented in paper Górski and Chmielewski (2008).

In last years, the random vibration method to evaluate the wind response of tall slender structures, which was outlined by Davenport (1962, 1964, 1967) and further developed by Harris (1965), is appreciate by researchers of the wind engineering again (Vickery 1995, Floris and Iseppi 2002, Pagnini and Solari 2002, Carassale and Solari 2002, Repetto and Solari 2002, Arunachalam and Lakshmanan 2008, Górski and Chmielewski 2008).

The paper is deals with a numerical study of the complete analysis of the dynamic cross-wind response of the 295 m-tall industrial chimney due to the turbulent wind flow. The influence of the vortex excitation, lateral turbulence component and motion-induced forces on the total cross-wind response of the chimney for different values of the wind velocity $\bar{u}_{10}$ has been investigated. Moreover, the influence of two damping ratios, evaluated by Multi-mode Random Decrement Technique, and number of natural mode shapes of the chimney have been considered. The random vibration method existing in literature have been applied to estimate three components mentioned above. Three power spectral density functions suggested by Kaimal, *et al*. (1972), Tieleman (1995) and Solari and Piccardo (2001) for the evaluation of the lateral response are taken into account. The vortex excitation response has been calculated by means of the Vickery and Basu's model including some complements. Motion-induced wind forces acting on a vibrating chimney have been modeled as a nonlinear aerodynamic damping force. Computer programmes have been developed to obtain responses of the chimney. The numerical results and their comparison are presented.

2. Description of the chimney and its structural parameters

The analyzed six-flue, 295 m-tall, industrial chimney is located in the Belchatow power station in Poland. The view, longitudinal section and cross-section of the chimney is shown in Fig. 1 a, c. This reinforced concrete chimney has structural shaft with different thicknesses of the wall along the height. The floor system is formed by a system of steel beams mainly within 36 m distance along the high. The chimney is placed on the circular foundation slab – 62.0 m in diameter (lying directly on the soil) which is 5.65 m high.

The measurements of the concrete strength of the shaft in compression on cylinders with 7.5 cm and 15 cm in diameter, were evaluated in 2001. Samples of the concrete were taken from the different height of the chimney. The mean value strength of these 40 samples was $f_{cm} = 24.2$ MPa.

The modulus of elasticity *E* of the concrete shaft was calculated, according to the Polish Standard (2002), from the formula

$$E = 11000 \cdot f_{cm}^{0.3} = 11000 \cdot 24.2^{0.3} \cong 29000 \text{ MPa}. \tag{1}$$

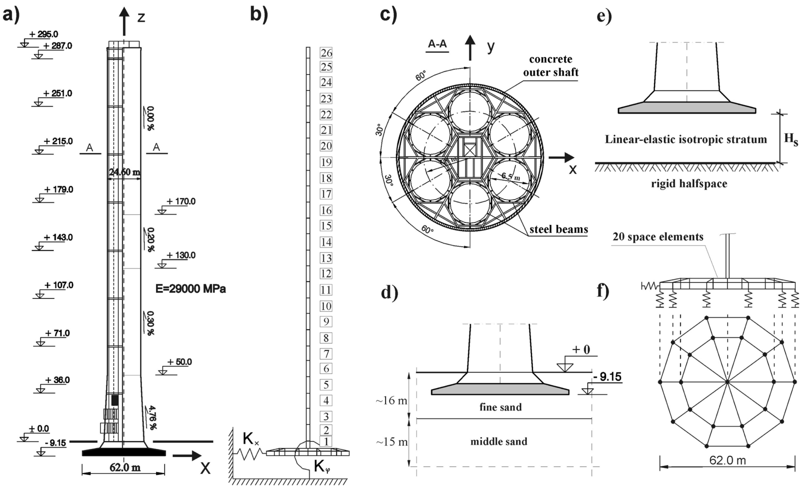

Fig. 1 Industrial chimney of Belchatow power station: (a) view and longitudinal section, (b) subdivision of the chimney into elements with soil springs, (c) cross-section, (d) description of the soil under foundation, (e) model of the soil under foundation to evaluate soil springs, (f) subdivision of the foundation slab

The description of the soil under foundation slab is given in Fig. 1d. Properties of the soil were tested in 1977 on the basis of thirteen drillings taken around the foundation of the chimney and real geotechnical conditions were taken into account.

The value of damping ratio of the chimney has been evaluated by Random Decrement Method. For that purpose, in the morning of 28th September 2007 from 9:00 to 11:00, the dynamic displacements of the chimney caused by weak wind were measured continuously (in cooperation with researchers from Stuttgart University of Applied Sciences in Germany) using Global Positioning System (GPS) technology. Procedure and application of GPS technology to measurements of displacements of tall slender structures is described in paper Breuer, *et al.* (2002, 2008) in detail.

The Kinematic method (Kinematic On the Fly - KOF) was applied to monitor dynamic displacements of the chimney. Using GPS Leica Geosystems 1200 equipment with two Dual Frequency Receivers (Reference and Rover Station) the satellite signals were tracked with a data rate of 0.5 second. This data rate is appropriate to analyze vibration with an expected frequency of about 0.2 Hz. The Reference Station was mounted on a tripod close to the entrance of the Belchatow power station. The Rover Station was installed at the most southerly point of the top of the chimney (295 m above the ground level). The lengths of the inclined baselines between two stations were 555 m. The chimney displacements were processed using the Post-Processing Kinematic Mode (PPK-GPS). Originally, on both stations the data were recorded for GPS post-processing using the static mode. Applying the RINEX format, datas can be prepared for kinematic post-processing which provided about 14400 chimney positions at 0.5 second intervals from two-hours measurements.

Preliminary the Random Decrement Method - RD (Tamura and Suganuma 1996, Ku, *et al.* 2007, Campbell, *et al.* 2007) has been used to determine the value of damping ratio of the chimney. The Random Decrement Method is a time domain method in which the structural response is transformed into random decrement function proportional to the correlation functions of the system operational response. The random decrement function (random decrement signature) can be ranked by the peak amplitude as follows (Tamura and Suganuma 1996)

$$a(R;\tau) = \frac{1}{N}\sum_{i=1}^{N} \operatorname{sgn}[x(t_i)]x(t_i+\tau)\Big|_{\dot{x}(t_i)=0,\,x(t_i)\in R} \tag{2}$$

where $x(t)$ is the response of the structure, sgn[x] is the sign of x, N is the number of ranks and R is the range of the peak value of $x(t)$.

The method is effective only for structures with well-separated vibration modes and needs to remove the components of the response not concerned with the fundamental natural frequencies (the band-pass filter from 0.18 to 0.25 Hz has been used in the calculation). The Random Decrement Method has provided two values of damping ratio in the x and y directions of the chimney (see Fig. 1c), respectively $\xi_x = 0.9\%$ and $\xi_y = 1.7\%$. These values are different because the cross-section of the chimney is bisymmetrical.

In the second approach, more accurate analysis based on the Multi-mode Random Decrement Method – MRD (Tamura, *et al.* 2005) has been investigated. The method is proposed to evaluate the damping ratio for structures with multiple closely spaced vibration modes. The random decrement signature is approximated by superimposing different damped free oscillations as follows

$$a_i(\tau) = \frac{x_{0i}}{\sqrt{1-\xi_i^2}}e^{-\xi_i\omega_i\tau}\cos(\sqrt{1-\xi_i^2}\,\omega_i\tau-\phi_i), \quad a(\tau) = \sum_{i=1}^{N} a_i(\tau)+m \tag{3}$$

where $a(\tau)$ is the random decrement signature, $a_i(\tau)$ is the random decrement signature for the ith mode component, x_{0i} is the initial value of ith mode component, ω_i is the ith mode natural undamped circular frequency, ϕ_i is the phase shift and m is the mean value correction of the random decrement signature.

Analysis based on the Multi-mode Random Decrement Method has given the following values of damping ratio in both directions: $\xi_x = 0.4\%$ and $\xi_y = 0.8\%$. These values are rational and have been taken into account in the computation of the cross-wind response of the chimney.

3. Calculation model and free vibrations of the chimney with flexibility of soil

The chimney has been idealised as an elastic, linear, homogeneous beam connected to the foundation (treated as 3-dimensional body) resting on the soil stratum of the finite depth over a rigid halfspace. The part of the chimney above the foundation was modeled as a 1-dimensional body divided into 26 beam elements (see Fig. 1b) undergoing axial deformation in order to formulate the stiffness element matrices. For these beam elements mass element matrices were formulated by the lumped mass approach. In the system mass matrix the mass of reinforced concrete shaft, mass floors and six inner flues were included. The foundation of the chimney was divided into 20 space elements (see Fig. 1f) with 8 nodes for each element (SOLID elements in accordance with the SAP90+ computer program).

The description of the underlying soil (under the circular foundation slab of the chimney) is shown in Fig. 1d. It has been applied the model of soil which is given in paper Chmielewski, *et al.* (2005) and is shown in Fig. 1e. For engineering purposes, in case of circular foundation with a radius R_0, resting on a soil stratum of the finite depth H_s over a rigid halfspace, Kausel (1974) proposed the following approximate expressions for the soil spring constant – see Fig. 1 (for $H_s/R_0 \geq 2$)

$$K_x = \frac{8GR_0}{2-\nu}\left(1+\frac{R_0}{2H_s}\right), \quad K_\varphi = \frac{8GR_0^3}{3(1-\nu)}\left(1+\frac{R_0}{6H_s}\right) \tag{4}$$

where G is the shear modulus of soil, ν is a Poisson ratio.

The system stiffness and the system mass matrices **K** and **M** have been evaluated based on the model of the chimney described above. The first four natural vibration frequencies and four natural mode shapes of the chimney with flexibility of soil were calculated using SAP90+ and numerical results are given in Fig. 2.

4. Turbulence modeling

The calculation of the wind excited response of slender structures requires a modeling of the wind field.

Let x, y, z be a Cartesian reference system with origin O on the ground; z is vertical and directed upwards. The wind field is decomposed into its average component vector and the fluctuating vector around the mean, Solari and Piccardo (2001). In this case the wind velocity vector at point x, y, z may be written as (see Fig. 3)

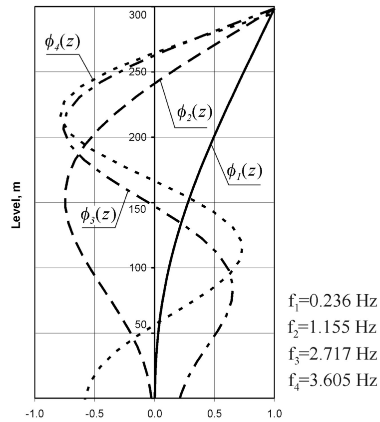

Fig. 2 The first four natural mode shapes and natural vibration frequencies of the chimney with flexibility of soil

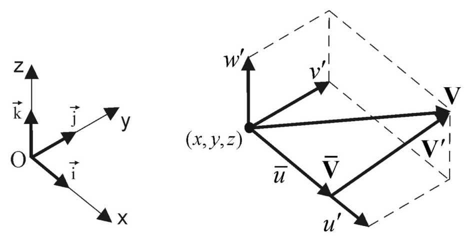

Fig. 3 Average component vector and the fluctuating vector of the wind velocity field

$$\mathbf{V}(x, y, z, t) = \bar{\mathbf{V}}(x, y, z) + \mathbf{V}'(x, y, z, t) \tag{5}$$

where t is the time, $\bar{\mathbf{V}}$ is the mean wind velocity vector and $\mathbf{V}'$ is the turbulent fluctuation vector (zero mean).

Considering a flat homogeneous terrain and the internal boundary layer, they are given by

$$\bar{\mathbf{V}}(x, y, z) = \vec{\mathrm{i}}\bar{u}(z) \tag{6}$$

$$\mathbf{V}'(x, y, z, t) = \vec{\mathrm{i}}u'(x, y, z, t) + \vec{\mathrm{j}}v'(x, y, z, t) + \vec{\mathrm{k}}w'(x, y, z, t) \tag{7}$$

where $\vec{\mathrm{i}}, \vec{\mathrm{j}}, \vec{\mathrm{k}}$ are the unit vectors in the directions x, y, z, $\bar{u}(z)$ is the mean wind velocity along with x; u', v', w' are the longitudinal (x), lateral (y) and vertical (z) turbulence components.

In the paper Solari and Piccardo (2001) the probabilistic 3-D turbulence model is proposed which is suited for carrying out response analyses of the wind-excited behaviour of vertical structures (buildings, chimneys, towers). Suitable spectral equations in this paper are given. They have been applied to evaluate the response of the industrial chimney due to the lateral turbulence component.

Assuming that the wind velocity and the wind direction is average in the time interval, the wind velocity field is considered as a stochastic stationary process for which probabilistic characteristics are unchangeable in a horizontal plane. Therefore in the time interval the turbulent fluctuation vector $\mathbf{V}'$ only depends on the height z above the ground:

$$\mathbf{V}'(x, y, z, t) = \vec{\mathrm{i}}u'(z, t) + \vec{\mathrm{j}}v'(z, t) + \vec{\mathrm{k}}w'(z, t) \tag{8}$$

Such assumption is typical for many practical applications and have been applied to evaluate the cross-wind response of the chimney.

5. Components of the cross-wind force

In case of a turbulent wind flow around a tall chimney with circular cross-section three components of the wind force are sources of the dynamic cross-wind response: (a) the lateral wind force due to the lateral turbulence component of the wind velocity field, (b) the vortex shedding wind force and (c) the motion-induced wind force. The chimney is a typical line-like structure, with a single spatial coordinate z. The total cross-wind force $W(z, t)$ per a unit length along the chimney may be written as

$$W(z, t) = W_v(z, t) + W_y(z, t) + W_m(z, t) \tag{9}$$

where $W_v(z, t)$ is the lateral wind force, $W_y(z, t)$ is the vortex shedding wind force and $W_m(z, t)$ is the motion-induced wind force.

6. Lateral turbulence component response of the chimney

6.1. Relationship between the spectrum of the lateral-wind force and the spectrum of the wind velocity

For lateral wind force $W_v(z, t)$, applying the quasi-steady and 'strip' assumptions, which relate the forces on a section of the chimney with the flow condition upstream of the section, one can write it as

$$W_v(z,t) = \frac{1}{2}\rho C_y(z)d(z)v(z,t)\bar{u}(z) \tag{10}$$

where $C_y(z)$ is the local drag coefficient, $d(z)$ is the local diameter and ρ is the air density.

If the chimney moves, this should be a relative velocity, which generates an aerodynamic force. However, at this point it will be assumed that the chimney is stationary.

It is assumed that the fluctuating component $v(z,t)$ is treated as a weakly stationary random process with respect to time t. Therefore, taking the means (time averages) of both sides of the joint moment of $W_v(z_1,t)\cdot W_v(z_2,t+\tau)$ we get

$$\overline{W_v(z_1,t)\cdot W_v(z_2,t+\tau)} = \frac{1}{4}C_y(z_1)C_y(z_2)d(z_1)d(z_2)\rho^2\bar{u}(z_1)\bar{u}(z_2)\overline{[v(z_1,t)v(z_2,t+\tau)]}\,. \tag{11}$$

This can be simplified for the uniform cross-section of the chimney, with $C_y(z)$ and $d(z)$ constants with z

$$\overline{W_v(z_1,t)\cdot W_v(z_2,t+\tau)} = \left(\frac{1}{2}C_y d\rho\right)^2\bar{u}(z_1)\bar{u}(z_2)\overline{[v(z_1,t)v(z_2,t+\tau)]} \tag{12}$$

After applying the Fourier transformation to Eq. (12), the fluctuation lateral wind-force spectrum $S_{W_v}(z_1,z_2,f)$ may be expressed in the form

$$S_{W_v}(z_1,z_2,f) = \left(\frac{1}{2}C_y d\rho\right)^2\bar{u}(z_1)\bar{u}(z_2)S_v(z_1,z_2,f) \tag{13}$$

where $S_v(z_1,z_2,f)$ is the cross spectrum of the fluctuating component of the lateral velocity, which can be expressed in terms of the power spectrum of the fluctuating component and the coherence function

$$S_v(z_1,z_2,f) = \sqrt{S_v(z_1,f)}\sqrt{S_v(z_2,f)}Coh(z_1,z_2,f) \tag{14}$$

If we assume that the fluctuating component $v(z,t)$ is a weakly homogeneous random process with respect to z, then Eq. (14) can be written as

$$S_v(z_1,z_2,f) = S_v(f)exp\left(\frac{-2kf|z_2-z_1|}{\bar{u}(z_1)+\bar{u}(z_2)}\right) \tag{15}$$

where k is the empirical constant, used to fit to the measured data; a typical value for the atmospheric turbulence is 6.5 (Solari and Piccardo 2001), $S_v(f)$ is the spectra density function for $v(z,t)$.

To describe the component of the lateral turbulence three power spectral density functions are taken into account as follows:

- Kaimal's power spectral density, Kaimal, *et al.* (1972)

$$S_v(z,f) = \frac{\bar{u}_{10}^2K}{f}\cdot\frac{17\bar{n}}{(1+9.5\bar{n})^{5/3}} \tag{16}$$

- Tieleman's power spectral density, Tieleman (1995)

$$S_v(z,f) = \frac{\bar{u}_{10}{}^2 K}{f} \cdot \frac{6.83\beta_v \bar{n}}{(1 + 75.84\bar{n}^{5/3})} \tag{17}$$

- Solari's power spectral density, Solari and Piccardo (2001), (d_v=9.434, λ_v=0.25)

$$S_v(z,f) = \frac{9.434\beta_v \bar{u}_{10}{}^2 K}{f} \cdot \frac{x}{(1 + 14.151x)^{5/3}} \tag{18}$$

where K is the roughness factor, $\bar{u}_{10}$ is the reference wind velocity, $x = f \cdot L_v(z)/\bar{u}(z)$, $\bar{n} = f \cdot z/\bar{u}(z)$, $\beta_v = 3.375 - 0.619\mathrm{arctg}[\ln(z_0) + 1.75]$, $L_v(z) = 75\left(\frac{z}{200}\right)^{\psi}$ is the length scale, $\psi = 0.67 + 0.05\ln(z_0)$ and z_0 is the roughness length.

Fig. 4 shows the comparison of power spectral density functions given in Eqs. (16), (17) and (18) for $\bar{u}_{10}$ = 18 m/s and z = 190 m.

6.2. Lateral-wind response of the chimney – random vibration approach

The dynamic response of the chimney due to the dynamic forces can be evaluated by the modal analysis. The complete displacement response $q_v(z, t)$ expands as a summation of components associated with each of the natural modes of vibration

$$q_v(z, t) = \sum_{i=1}^{N} y_i(t)\phi_i(z) \tag{19}$$

where $\phi_i(z)$ is the mode shape for the ith mode, $y_i(t)$ is a time-varying generalized coordinate and z is a spatial coordinate on the chimney.

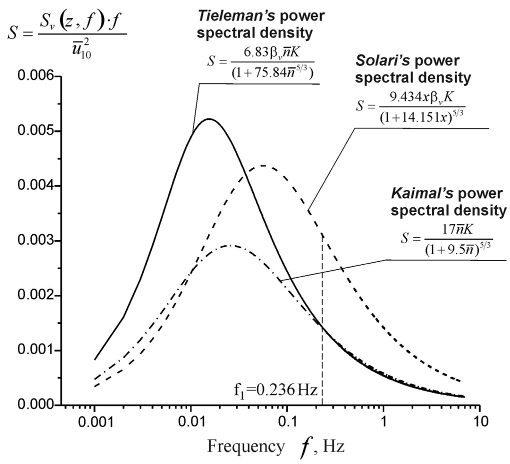

Fig. 4 Comparison of power spectral density functions of the lateral turbulence component for $\bar{u}_{10}$ = 18 m/s and z = 190 m

The modal analysis of the chimney has been evaluated and is presented in book (Chmielewski and Zembaty 1998). The equation of motion for the i*th* generalized coordinate is as follows

$$M_i\ddot{y}_i(t) + 2\xi_i\omega_i M_i\ddot{y}_i(t) + K_i y_i(t) = P_{vi}(t) \tag{20}$$

where M_i is the generalized mass equal to $\int_0^H m(z)\phi_i^2(z)dz$, $m(z)$ is the mass per a unit length along the chimney, H is the height of the chimney, ξ_i is the damping ratio for the i*th* mode, ω_i is the natural undamped circular frequency for the i*th* mode, K_i is the modal stiffness and $P_{vi}(t)$ is the generalized force equal to $\int_0^H W_v(z,t)\phi_i(z)dz$ fluctuating along the wind force.

The spectral density of $P_{vi}(t)$ can be obtained in an analogous way to the mean square value of $W_v(z, t)$, it is as follows (Fig. 5a)

$$S_{P_{vi}}(f) = \int_0^H\int_0^H S_{W_v}(z_1, z_2, f)\phi_i(z_1)\phi_i(z_2)dz_1dz_2\,. \tag{21}$$

Based on the random vibration theory (Chmielewski and Zembaty 1998), the spectral density of the generalized coordinate $y_i(t)$ is given by (Figs. 8 and 11)

$$S_{y_i}(f) = \frac{1}{M_i^2}|H_i(f)|^2 S_{P_{vi}}(f) \tag{22}$$

where the mechanical admittance for the i*th* mode is (Fig. 5b)

$$|H_i(f)|^2 = \frac{1}{(2\pi f_i)^4\left\{\left[1-\left(\frac{f}{f_i}\right)^2\right]^2 + 4\xi_i^2\left(\frac{f}{f_i}\right)^2\right\}} \tag{23}$$

where f_i is the i*th* natural frequency.

The mean square value of $y_i(t)$ can be obtained by integrating Eq. (22) with respect to frequency

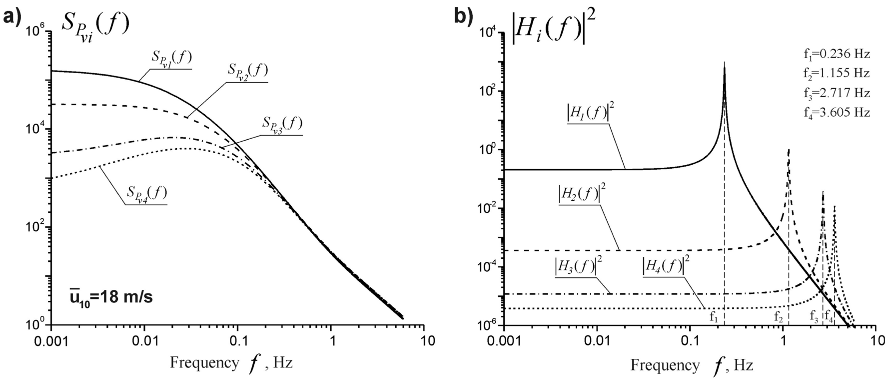

Fig. 5 (a) Power spectral density function of the generalized force due to the lateral turbulence component for first four natural frequencies of the chimney ($\bar{u}_{10}$ = 18 m/s, z = 190 m), (b) mechanical admittance for the first four natural frequencies of the chimney (ξ_y = 0.8%)

$$\overline{y_i^2} = \int_0^{\infty} S_{y_i}(f)df. \tag{24}$$

Applying Eq. (19), the mean square displacement is obtained from

$$\sigma_{qv}^2(z) = \sum_{i=1}^{N}\sum_{k=1}^{N} \overline{y_i y_k}\phi_i(z)\phi_k(z). \tag{25}$$

The cross-coupling between modes for the chimney can be neglected, the above equation becomes

$$\sigma_{qv}^2(z) = \sum_{i=1}^{N} \overline{y_i^2}\phi_i^2(z). \tag{26}$$

The mean square value of any other response (e.g. bending moment, stress) can similarly be obtained. Computer programmes were developed to obtain the lateral response of the six-flue, 295 m-tall chimney and results of calculation for damping ratio $\xi_y = 0.8\%$ are given below.

Fig. 6 shows rms values of lateral displacements and bending moments of the chimney due to the lateral turbulence component for $\bar{u}_{10} = 18$ m/s. The comparison of the rms lateral wind displacements of the top of the chimney for the different reference wind velocity $\bar{u}_{10}$ are shown in Fig. 7.

The influence of the number of natural vibration frequencies and natural mode shapes of the chimney on the lateral wind response has been investigated. Fig. 8 depicts the comparison of considered three power spectral density functions of the lateral turbulence component response of the chimney for the first and first four natural frequencies. Table 1 and 2 contains the comparison of

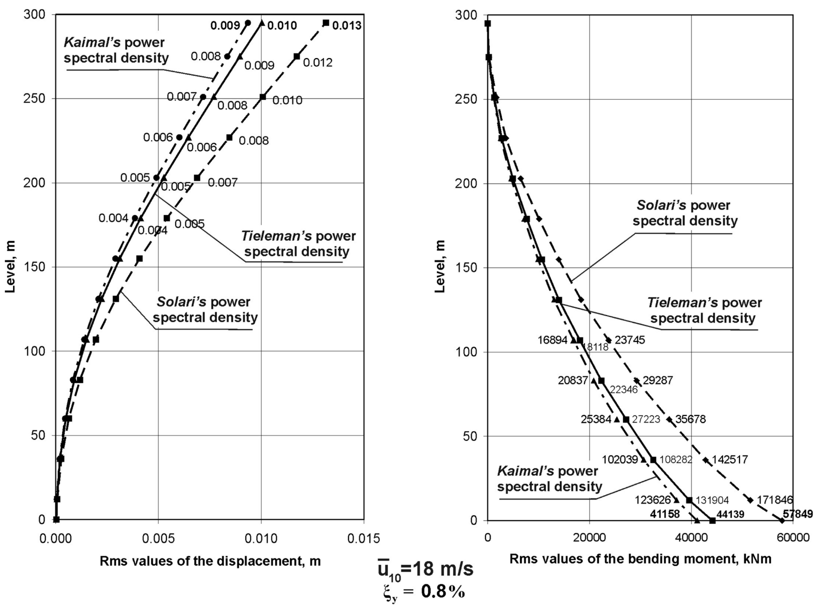

Fig. 6 Comparison of rms values of displacements and bending moments of the chimney due to the lateral turbulence component for $\bar{u}_{10} = 18$ m/s

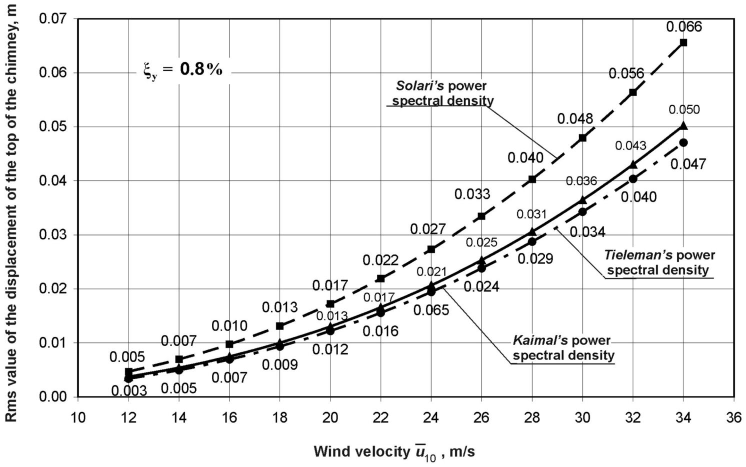

Fig. 7 Comparison of rms values of lateral displacements of the top of the chimney due to the lateral turbulence component for different values of $\bar{u}_{10}$

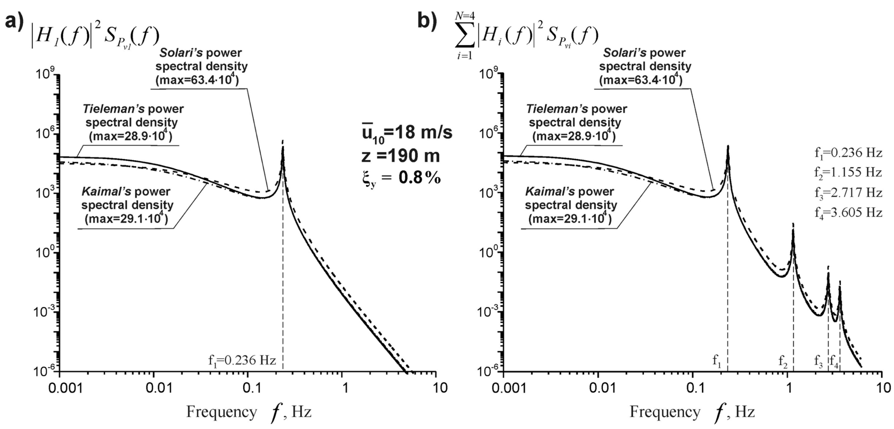

Fig. 8 Comparison of power spectral density functions of the lateral turbulence component response of the chimney for (a) the first and (b) first four natural frequencies of the chimney

rms values of displacements of the chimney due to the lateral turbulence component for the first and first four natural frequencies of the chimney.

7. Vortex-wind response of the chimney

7.1. Vortex-wind force and spectrum of vortex-induced force

The phenomena of separating shear layers and vortex shedding for a bluff body with the circular cross-section is well described. For the chimney with the Reynolds number generally in excess of 10^7 the flow regimes for a circular cylinder are called post-critical. These flow regimes are turbulent and the alternate shedding of vortices induces a random cross-wind force on the chimney. A random excitation model, for the vortex shedding response prediction, which was developed by Vickery and

Table 1 Comparison of rms values of displacements of the chimney due to the lateral turbulence component for first four natural mode shapes of the chimney and $\bar{u}_{10}$ = 18 m/s

Level z (m)	Rms values of displacements of the chimney due to the lateral turbulence component $\sigma_{qv}(z)$ (cm)				$\frac{\text{col.5} - \text{col.2}}{\text{col.2}} \cdot 100$ (%)
	first natural mode shape	first two natural mode shapes	first three natural mode shapes	first four natural mode shapes	
1	2	3	4	5	6
295	1.31472	1.31486	1.31487	1.31487	0.011
275	1.17284	1.17291	1.17291	1.17291	0.006
251	1.00771	1.00772	1.00772	1.00772	0.001
228	0.84551	0.84551	0.84552	0.84552	0.001
203	0.68886	0.68892	0.68892	0.68892	0.009
155	0.54156	0.54171	0.54171	0.54171	0.028
131	0.40811	0.40836	0.40836	0.40836	0.062
107	0.29209	0.29242	0.29242	0.29242	0.113
179	0.19509	0.19544	0.19544	0.19544	0.182
83	0.11820	0.11851	0.11852	0.11852	0.272
60	0.06377	0.06400	0.06401	0.06401	0.386
36	0.02691	0.02705	0.02706	0.02706	0.580
12	0.00748	0.00756	0.00758	0.00759	1.485
0	0.00243	0.00249	0.00253	0.00259	6.551

Table 2 Comparison of rms values of lateral displacements of the top of the chimney due to the lateral turbulence for first four natural mode shapes of the chimney for different values of $\bar{u}_{10}$

Wind velocity $\bar{u}_{10}$ (m/s)	Rms values of displacements of the top of the chimney due to the lateral turbulence component $\sigma_{qv}(z)$ (cm)				$\frac{\text{col.5} - \text{col.2}}{\text{col.2}} \cdot 100$ (%)
	first natural mode shape	first two natural mode shapes	first three natural mode shapes	first four natural mode shapes	
1	2	3	4	5	6
12	0.47117	0.47123	0.47123	0.47123	0.013
14	0.69487	0.69495	0.69495	0.69495	0.013
16	0.97469	0.97480	0.97480	0.97480	0.012
18	1.31472	1.31486	1.31487	1.31487	0.011
20	1.71862	1.71880	1.71880	1.71880	0.010
22	2.18957	2.18979	2.18979	2.18979	0.010
24	2.73040	2.73066	2.73066	2.73066	0.010
26	3.34353	3.34384	3.34384	3.34384	0.009
28	4.03119	4.03156	4.03156	4.03156	0.009
30	4.79518	4.79561	4.79562	4.79562	0.009
32	5.63721	5.63771	5.63772	5.63772	0.009
34	6.55864	6.55921	6.55922	6.55922	0.009

Basu (1983), has been applied. According to this model, the vortex shedding wind force per a unit length may be written as

$$W_y(z,t) = \frac{1}{2}\rho d(z)\bar{u}^2(z)C_L(z,t) \tag{27}$$

where $C_L(z, t)$ is a non-dimensional, normalized lift coefficient. $C_L(z, t)$ is a weakly stationary random process with zero mean.

The Vickery and Basu's model is a semi-empirical mathematical model which has been presented for predicting the cross-wind response of tall slender structures of circular cross-section to the wind. In this model the forces caused by vortex shedding are characterized by four aerodynamic parameters; the lift coefficient $C_L(z, t)$, the spectral bandwidth, the Strouhal number and a measure of the spanwise correlation. The following section concerns with the definition of the key parameters for circular cross-sections in large scale turbulence and at the Reynolds numbers consistent with full scale structures.

The spectrum of the normalized lift force $S_{CL}(z, f)$ per a unit length (Fig. 9a) is expressed as

$$\frac{fS_{CL}(z,f)}{\sigma_{CL}^2(z)} = \frac{f}{\sqrt{\pi}B(z)f_s(z)}\exp\left[-\left[\frac{1-\frac{f}{f_s(z)}}{B(z)}\right]^2\right] \tag{28}$$

where f_s is the shedding frequency, B is the bandwidth parameter which is expressed by the relationship $B(z) = 0.1 + 2.0\ I(z)$, $St = f_s d(z)/\bar{u}(z)$ is the Strouhal number, and σ_{CL} is the rms of the normalized lift force per a unit length equal to Vickery and Basu (1983), and Waldeck (1992)

$$\sigma_{CL}(z) = [0.15 + 0.55I^*(z)] - [0.09 + 0.55I^*(z)]e^{-(20I^*(z))^3} \tag{29}$$

where $I^*(z)$ is the modified turbulence intensity given by

$$I^*(z) = I(z)\left(\frac{d(z)}{L(z)}\right)^{\frac{1}{3}} \tag{30}$$

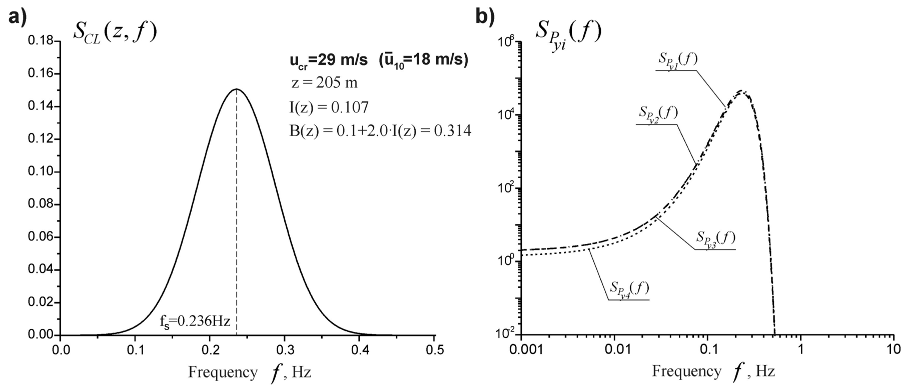

Fig. 9 (a) Spectrum of the normalized lift vortex force per a unit length, (b) power spectral density function of the generalized vortex force for first four natural frequencies of the chimney

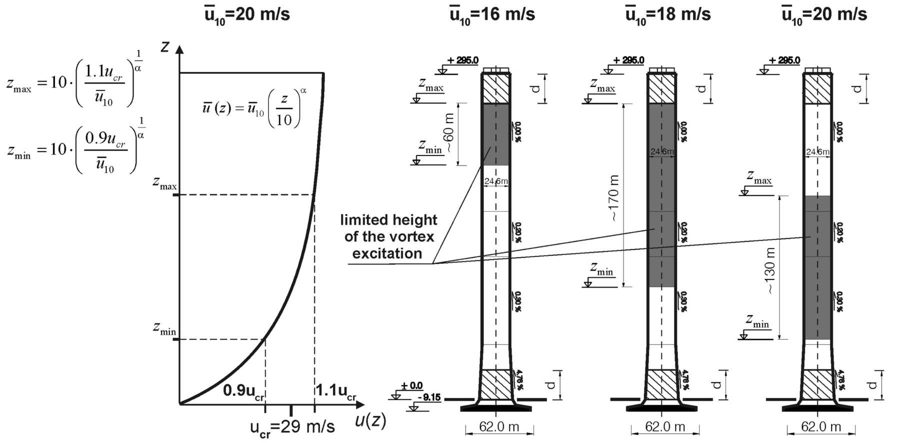

Fig. 10 Assumption of the limited height of the vortex excitation for different values of $\bar{u}_{10}$

where $L(z)$ is the integral length scale of turbulence and $I(z)$ is the turbulence intensity

$$I(z) = \frac{\sigma_{u'}(z)}{\bar{u}(z)} \tag{31}$$

The integral length scale $L(z)$ at heights of z in the range of 10-240 m has been suggested by Counihan (1975) in the form

$$L(z) = Cz^m \tag{32}$$

where C and m depend on the roughness length z_0.

It has been assumed that the vortex excitation may occur on the limited height of the chimney which corresponds to the mean wind velocity $\bar{u}(z) \in \langle 0.9u_{cr}; 1.1u_{cr}\rangle$ and with the exception of two boundary zones; near the base and near the free end of the chimney where vortex excitation is disturb – see Fig. 10.

7.2. Vortex-wind response of the chimney – random vibration approach

The dynamic vortex-wind response of the considered chimney was evaluated in the same manner as described in section concern the lateral-wind response, i.e. by the modal analysis.

On the basis of the random vibration approach the mean square value of the displacement $\sigma^2_{qy}(z)$ becomes

$$\sigma^2_{qy}(z) = \sum_{i=1}^{N}\left(\frac{\phi_i(z)}{M_i}\right)^2 \int_0^{\infty} S_{P_{yi}}(f)\left|H_i(f)\right|^2 df \tag{33}$$

where the power spectral density function of the generalized vortex force $S_{P_{yi}}(f)$ is given in the form – see Fig. 9 b

$$S_{P_{yi}}(f) = \frac{\rho^2}{4}\int_0^H\int_0^H d(z_1)d(z_2)\bar{u}^2(z_1)\bar{u}^2(z_2)S_{CL}(z_1, z_2, f)\phi_i(z_1)\phi_i(z_2)dz_1dz_2 \tag{34}$$

where $S_{CL}(z_1, z_2, f)$ is the cross spectrum of the vortex-induced force suggested by Vickery and Basu (1983) in the form

$$S_{CL}(z_1, z_2, f) = \sqrt{S_{CL}(z_1, f)}\sqrt{S_{CL}(z_2, f)}R(z_1, z_2), \tag{35}$$

$$R(z_1, z_2) = \cos\left(\frac{2r}{3}\right)\exp\left\{-\left(\frac{r}{3}\right)^2\right\} \tag{36}$$

and r is the dimensionless distance

$$r = \frac{2(z_1 - z_2)}{d(z_1) + d(z_2)}. \tag{37}$$

The maximum vortex shedding displacements of the chimney is expressed as

$$q_v(z) = g \cdot \sigma_{qv}(z) \tag{38}$$

where g is the peak factor (g = 3.33).

Fig. 11 shows the comparison of power spectral density functions of the vortex excitation and lateral turbulence component response of the chimney for $\bar{u}_{10}$ = 18 m/s and $\bar{u}_{10}$ = 24 m/s.

The comparison of the maximum vortex shedding displacements of the chimney for $\bar{u}_{10}$ = 18 m/s (corresponding to the critical wind velocity u_{cr} = 29 m/s) computed for two values of damping ratio ξ_x = 0.4% and ξ_y = 0.8% is shown in Fig. 12.

8. Cross-wind response caused by structural motion

Let assume that the chimney is moving. In this case a relative wind velocity generates a nonlinear aerodynamic damping force proportional to the velocity of the structure $\dot{q}_y(z, t)$. Let $W_m(z, t)$ be the force per a unit length along the chimney as the motion-induced wind force in the form (Vickery 1994)

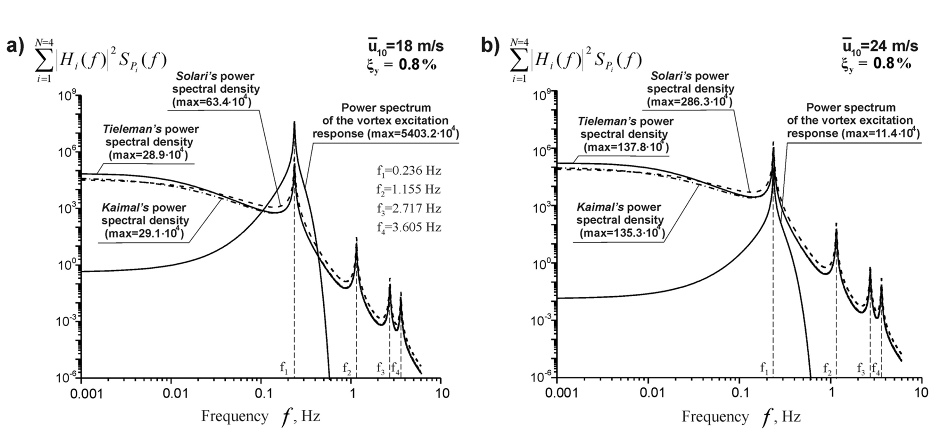

Fig. 11 Comparison of power spectral density functions of the vortex excitation and lateral turbulence component response of the chimney for $\bar{u}_{10}$ = 18 m/s (a) and $\bar{u}_{10}$ = 24 m/s (b)

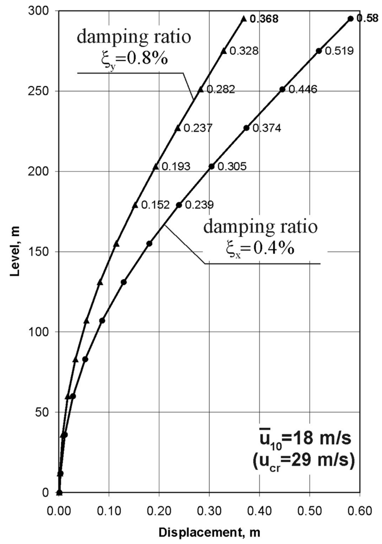

Fig. 12 Comparison of the vortex excitation response of the chimney for $\xi_y = 0.8\%$ and $\xi_x = 0.4\%$

$$W_m(z,t) = 4\pi f_i \rho d^2(z) K_a(z) \dot{q}_y(z,t) \tag{39}$$

where

$$K_a(z) = K_{ao}(z)\left[1 - \left(\frac{\sigma_{qy}(z)}{\alpha d(z)}\right)^2\right] \tag{40}$$

$K_{ao}(z)$ is the aerodynamic damping parameter which has been measured in a turbulent wind flow for circular cylinder and is given in paper (Vickery 1995), and $\alpha d(z)$ is the limiting cross-wind displacement ($\alpha \cong 0.4$).

If we take into account aeroelastic effects as a nonlinear aerodynamic damping force the equation of motion for the *ith* generalized coordinate is as follows

$$M_i \ddot{y}_i(t) + 2\xi_{si}\omega_i M_i \dot{y}_i(t) + K_i y_i(t) = P_{yi}(t) + 4\pi f_i \rho \kappa_i \dot{y}_i(t) \tag{41}$$

where κ_i is the modal aerodynamic damping parameter equal to $\int_0^H K_a(z) d^2(z) \phi_i^2(z) dz$.

After transformation and division by M_i, Eq. (41) can be written as

$$\ddot{y}_i(t) + 2\omega_i(\xi_{si} + \xi_{ai})\dot{y}_i(t) + \omega_i^2 y_i(t) = \frac{P_{yi}(t)}{M_i} \tag{42}$$

where $\xi_{ai} = -\frac{\rho\kappa_i}{M_i}$ is the modal aerodynamic damping ratio for the *ith* mode.

The mean square value of the displacement $\sigma_{qy}^{2}{}^*(z)$ of the vibrating chimney becomes

$$\sigma_{qy}^{2}{}^*(z) = \sum_{i=1}^{N} \left(\frac{\phi_i(z)}{M_i}\right)^2 \int_0^\infty S^*_{P_{yi}}(f) \left|H_i^*(f)\right|^2 df \tag{43}$$

where the power spectral density function of the generalized force is given in the form

$$S^*_{P_{yi}}(f) = \frac{\rho^2}{4}\int_0^H\int_0^H d(z_1)d(z_2)\bar{u}^2(z_1)\bar{u}^2(z_2)\sqrt{S_{CL}(z_1,f)}\sqrt{S_{CL}(z_2,f)}R_y(z_1,z_2)\phi_i(z_1)\phi_i(z_2)dz_1dz_2 \quad (44)$$

and the mechanical admittance for the ith mode depends on the value of $\sigma^*_{qy}(z)$

$$|H^*_i(f)|^2 = \frac{1}{(2\pi f_i)^4\left\{\left[1-\left(\frac{f}{f_i}\right)^2\right]^2+4\left(\frac{f}{f_i}\right)^2\left(\xi_s-\frac{\rho\kappa_i}{M_i}\right)\right\}} \quad (45)$$

and should be evaluated by an iteration technique.

The spanwise correlation function of the vortex shedding wind force of the vibrating chimney increase with increasing of the vibration amplitude of the structure and is suggested by Vickery and Basu (1983) as follows

$$R_y(z_1,z_2) = \frac{R(z_1,z_2)+\left(a(z)\frac{q_y(z)}{d(z)}\right)^2}{1+\left(a(z)\frac{q_y(z)}{d(z)}\right)^2} \quad (46)$$

where $R(z_1, z_2)$ is the spanwise correlation function of the stationary structure (Eq. (36) and Fig. 13) and

$$a(z) = 2\sqrt{2}\left(\frac{2\pi f_i d(z)}{\bar{u}(z)}\right)^2\frac{K_a(z)}{\sigma_{CL}(z)}. \quad (47)$$

The critical wind velocity of the vibrating chimney u^*_{cr} is greater than the critical wind velocity of the stationary chimney u_{cr} and is expressed as follows (Flaga 1997)

$$u^*_{cr}(z_{ref}) = \frac{f_i \cdot d_{ef}(z_{ref})}{St} \quad (48)$$

where $d_{ef}(z_{ref}) = d(z_{ref})+\alpha_c q_y(z_{ref})$ is the effective reference diameter of the vibrating chimney and α_c is the experimental parameter.

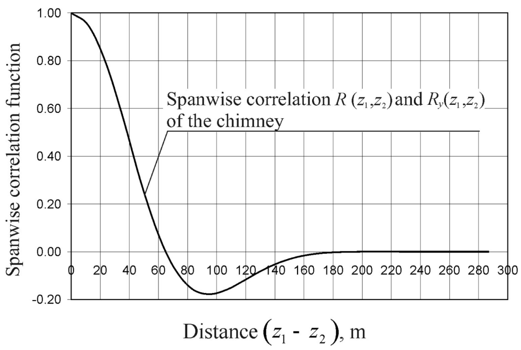

Fig. 13 Spanwise correlation function of the vortex shedding wind force of the chimney

9. Total cross-wind response of the chimney

If we assume that the vortex shedding and lateral-wind force are uncorrelated (Solari 1996), the total maximum cross-wind displacement of the chimney due to both excitations can be expressed as

$$q_{total}(z) = g(\sqrt{\sigma_{qv}^2(z) + \sigma_{qy}^2(z)}) \tag{49}$$

where $\sigma_{qv}(z)$ is the standard deviation of the lateral turbulence component displacement and $\sigma_{qy}(z)$ is the standard deviation of the vortex shedding displacement.

Based on the measurement results two different values of the damping ratio in the x and y directions of the chimney, respectively $\xi_x = 0.4\%$ and $\xi_y = 0.8\%$, have been evaluated. Fig. 14 and 15 depicts comparison of the top chimney lateral and vortex excitation displacements for the different reference wind velocity $\bar{u}_{10}$ and for two evaluated values of damping ratio.

For such different values of the damping ratio, the average wind direction acting on the chimney has a great significance on the wind response of the structure. If the wind flow along the y direction (considered value of the damping ratio is $\xi_x = 0.4\%$), the cross-wind response of the chimney is greater than the wind flow along the x direction (considered value of the damping ratio is $\xi_y = 0.8\%$). In this case for the sake of safety of the structure, the most disadvantageous wind direction should be consider for evaluation of the cross-wind response.

In the computations the following data have been used: $z_0 = 0.03$ m (the roughness length), K = 0.005 (the terrain factor depending on the roughness length), $\alpha = 0.16$ (the power law exponent for the mean wind speed profile), $C_D = 0.64$ (the drag coefficient), $g = 3.33$ (the peak factor), $\xi_{a1} = -0.00019$, $\xi_{a2} = -0.00026$, $\xi_{a3} = -0.00016$ and $\xi_{a2} = 0.00007$ (the aerodynamic damping for the first four mode shapes respectively), St = 0.2 (the Strouhal number), $\rho = 1.25$ kg/m^3 (the air density), $\nu = 0.145 \cdot 10^{-4}$ m^2/s (the kinematic viscosity of the air), $z_{ref} = 205$ m (the reference height of the chimney), $u_{cr} = \frac{f_1 \cdot d(z_{ref})}{St} = \frac{0.236 \cdot 24.6}{0.2} = 29.0\frac{m}{s}$ (the critical wind velocity of the stationary chimney which corresponds to the mean wind velocity $\bar{u}_{10} = 18$ m/s), $Re = \frac{d(z_{ref}) \cdot u_{cr}}{\nu} = \frac{24.6 \cdot 29.0}{0.145 \cdot 10^{-4}} = 4.92 \cdot 10^7$ (the Reynolds

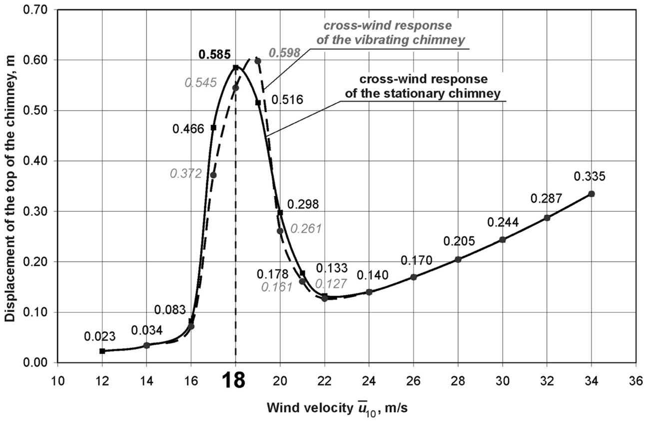

Fig. 14 Cross-wind response of the stationary and vibrating chimney due to the vortex excitation and lateral turbulence component for different values $\bar{u}_{10}$ of and damping ratio $\xi_x = 0.4\%$

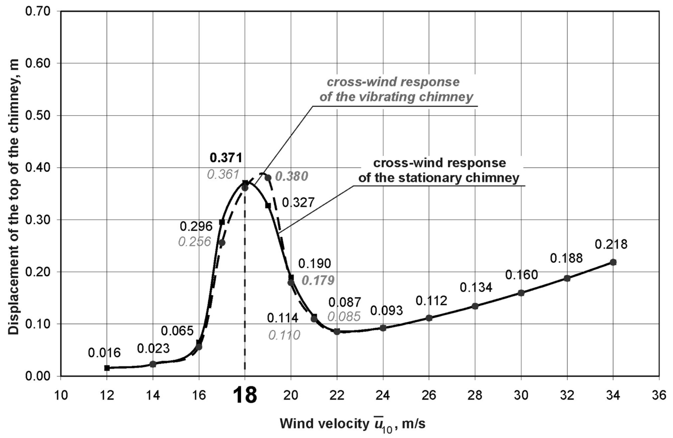

Fig. 15 Cross-wind response of the stationary and vibrating chimney due to the vortex excitation and lateral turbulence component for different values of $\bar{u}_{10}$ and damping ratio $\xi_y = 0.8\%$

number), $Sc = \dfrac{4 \cdot \pi \cdot \xi_s \cdot m}{\rho \cdot d^2(z_{ref})} = \dfrac{4 \cdot \pi \cdot 0.008 \cdot 73626.85}{1.25 \cdot 24.6^2} = 9.8$ (the Scruton number), $I(z_{ref}) = 2.45 \cdot \sqrt{K} \cdot \left(\dfrac{z_{ref}}{10}\right)^{-\alpha} = 2.45 \cdot \sqrt{0.005} \cdot \left(\dfrac{205}{10}\right)^{-0.16} = 0.11$ (the turbulence intensity at reference height of the chimney), $B(z_{ref}) = 0.1 + 2.0\ I(z_{ref}) = 0.32$ (the bandwidth parameter), $d_{ef}(z_{ref}) = 24.80$ m (the effective reference diameter of the vibrating chimney), $u^*_{cr}(z_{ref}) = \dfrac{f_1 \cdot d_{ef}(z_{ref})}{St} = \dfrac{0.236 \cdot 24.80}{0.2} = 29.3\dfrac{m}{s}$ (the critical wind velocity of the vibrating chimney).

10. Conclusions

1. The response of the chimney due to the lateral turbulence component depends on its power spectral density. The response computed according to the Solari's power spectral density is about 33% greater than for the Tieleman's power spectral density and about 42% greater than for the Kaimal's power spectral density. The results confirm that most significant for the power spectral density function of $v(z, t)$ are values corresponding to the eigenvalue frequency range of the structure. These values are greatest on the Solari's power spectral density (Fig. 4). The values of the eigenvalue frequency range are amplified by the mechanical admittance of the structure (Fig. 8).

2. The influence of the number of natural frequencies and natural mode shapes of the chimney on the lateral-wind response has been investigated. The influence of the first natural frequency and first natural mode shape on the lateral-wind response is greater than 99%. For the vortex excitation response only the first mode shape has been considered because the frequency range of the power spectral density of the vortex excitation is limited approximately to 0.6 Hz – see Fig. 11.

3. Based on the measurement results two different values of the damping ratio in the x and y directions of the chimney, respectively $\xi_x = 0.4\%$ and $\xi_y = 0.8\%$, have been evaluated. The total cross-wind response of the chimney computed for the damping ratio $\xi_x = 0.4\%$ is greater about 57%

than for the damping ratio $\xi_y = 0.8\%$. For such different values of the damping ratio, the average wind direction acting on the chimney has a great significance on the wind response of the structure. If the wind flow along the *y* direction (considered value of the damping ratio is $\xi_x = 0.4\%$), the cross-wind response of the chimney is greater than the wind flow along the *x* direction (considered value of the damping ratio is $\xi_y = 0.8\%$). In this case for the sake of safety of the structure, the most disadvantageous wind direction should be consider for evaluation of the cross-wind response.

4. The vortex shedding excitation has relevant influence on the cross-wind response of the chimney in the range of the wind velocities $\bar{u}_{10} = 16 \div 22$ m/s. The greatest vortex shedding response appears for $\bar{u}_{10} = 18$ m/s which corresponds to the critical wind velocity of about $u_{cr} = 29$ m/s. At this wind velocity the vortex shedding response is dominant and the influence of the lateral turbulence component on the total cross-wind response is limited to several percent.

5. The motion-induced wind forces acting on a vibrating chimney have been modeled as a nonlinear aerodynamic damping force. The critical wind velocity of the vibrating chimney is greater than the critical wind velocity of the stationary chimney. The influence of the motion-induced response for the critical wind velocity is about 2%.

References

Arunachalam, S. and Lakshmanan, N. (2008), "Studies on across-wind loads on a circular chimney", *Proc. of the 4th Int. Conf. on Advances in Wind and Structures*, Jeju, S. Korea, May 29-31, 2008, 851-862.

Breuer, P., Chmielewski, T., Górski, P. and Konopka, E. (2002), "Application of the GPS technology to measurements of displacements of high-rise structures due to weak winds", *J. Wind Eng. Ind. Aerod.*, **90**, 223-230.

Breuer, P., Chmielewski, T., Górski, P., Konopka, E. and Tarczyski, L. (2008), "The Stuttgart TV Tower - displacement of the top caused by the effects of sun and wind", *Eng. Struct.*, **30**, 2771-2781.

Campbell, S., Kwok, K.C.S., Hitchcock, P.A., Tse, K.T. and Leung, H.Y. (2007), "Field measurements of natural periods of vibration and structural damping of wind-excited tall residential buildings", *Wind Struct.*, **10**(5), 401-420.

Carassale, L. and Solari, G. (2002), "Wind modes for structural dynamics: a continuous approach", *Probabilist Eng. Mech.*, **17**, 157-166.

Chmielewski, T., Górski, P., Beirow, B. and Kretzschmar, J. (2005), "Theoretical and experimental free vibrations of tall industrial chimney with flexibility of soil", *Eng. Struct.*, **27**, 25-34.

Chmielewski, T. and Zembaty, Z. (1998), *Dynamics of Structures*, Arkady, Warsaw (in Polish).

Counihan, J. (1975), "Adiabatic atmospheric boundary layers: a review and analysis of data from the period 1880-1972", *Atmos. Environ.*, **9**, 871-905.

Davenport, A.G. (1962), "The response of slender, line-like structures to a gusty wind", *Proc. of the Institution of Civil Engineers*, **23**, 389-408.

Davenport, A.G. (1964), "Note on the distribution of the largest value of a random function with application to gust loading", *Proc. of the Institution of Civil Engineers*, **28**, 187-196.

Davenport, A.G. (1967), "Gust loading factors", *J. Struct. Div. ASCE*, **93**, 11-34.

Flaga, A. (1996), *Wind vortex-induced excitation and vibration of slender structures. Single structure of circular cross-section normal to flow*, Cracow University of Technology, Monograph No 202, Kraków.

Flaga, A. (1997), "Nonlinear amplitude dependent self-limiting model of lock-in phenomenon at vortex excitation", *J. Wind Eng. Ind. Aerod.*, **69-71**, 331-340.

Floris, C., Iseppi, L. (2002), "Stochastic along-wind response of nonlinear structures to quadratic wind pressure", *Wind Struct.*, **5**(5), 423-440.

Górski, P. and Chmielewski, T. (2008), "A comparative study of along and cross-wind responses of a tall chimney with and without flexibility of soil", *Wind Struct.*, **11**(2), 121-135.

Harris, R.I. (1965), "The random vibration of distributed parameter mechanical systems with reference to wind problems", *Elec. Res. Assoc. U.K. Rep. No 5110*.

Kaimal, J.C., Wyngaard, J.C., Izumi, Y. and Cotè, O.R. (1972), "Spectral characteristics of surface layer turbulence", *Q. J. Roy. Meteor. Soc.,* **98**, 563-589.

Kausel, E. (1974), *Res. Rep. R74-11*, Dept. Civ. Eng. M.I.T.

Ku, C.J., Cermak, J.E. and Chou, L.S. (2007), "Random decrement based method for modal parameter identification of a dynamic system using acceleration responses", *J. Wind Eng. Ind. Aerod.*, **95**, 389-410.

Pagnini, L.C. and Solari, G. (2002), "Gust buffeting and turbulence uncertainties", *J. Wind Eng. Ind. Aerod.*, **90**, 441-459.

PN-B-03264:2002 (2002), *Static computation and design.*

PREN 1991-1-4.6. (2003), *Eurocode 1: Actions on structures – Part 1-4: General actions – Wind actions.*

Repetto, P.M. and Solari, G. (2002), "Dynamic crosswind fatigue of slender vertical structures", *Wind Struct.*, **5**(6), 527-542.

Ruscheweyh, H. (1982), *Dynamic Action on Buildings*, Vol. II, Bauverlag, Wiesbaden, (in German).

Ruscheweyh, H. and Galemann, T. (1996), "Full-scale measurements of wind-induced oscillations of chimney", *J. Wind Eng. Ind. Aerod.*, **65**, 55-62.

Ruscheweyh, H., Hortmanns, M. and Schnakenberg, C. (1996), "Vortex-excited vibrations and galloping of slender elements", *J. Wind Eng. Ind. Aerod.*, **65**, 347-352.

Ruscheweyh, H., Langer, W. and Verwiebe, C. (1998), "Long-term full-scale measurements of wind induced vibrations of steel stacks", *J. Wind Eng. Ind. Aerod.*, **74-76**, 777-783.

Sanada, S., Suzuki, M. and Matsumoto, H. (1992), "Full scale measurements of wind force acting on a 200m concrete chimney, and the chimney's response", *J. Wind Eng. Ind. Aerod.*, **41-44**, 2165-2176.

Solari, G. (1996), "Evaluation and role of damping and periods for the calculation of structural response under wind loads", *J. Wind Eng. Ind. Aerod.*, **59**, 191-210.

Solari, G. and Piccardo, G. (2001), "Probabilistic 3-D turbulence modelling for gust buffeting of structures", *Probabilist Eng. Mech.*, **16**, 73-86.

Tamura, Y. and Suganuma, S. (1996), "Evaluation of amplitude-dependent damping and natural frequency of buildings during strong winds", *J. Wind Eng. Ind. Aerod.*, **59**, 115-130.

Tamura, Y., Yoshida, A. and Zhang, L. (2005), "Damping in buildings and estimation techniques", *Proc. of the 6th Asia-Pacific Conf. on Wind Engineering*, Seoul, S. Korea, Sept. 12-14, 2005, 193-214.

Tieleman, H.W. (1995), "Universality of velocity spectra", *J. Wind Eng. Ind. Aerod.,* **56**, 55-69.

Vickery, B.J. and Basu, R.I. (1983), "Across-wind vibrations of structures of circular cross-section", *J. Wind Eng. Ind. Aerod.,* **12**, Part I 49-73, Part II 75-97.

Vickery, B.J. (1994), "Across wind loading on reinforced concrete chimneys of circular cross section", *State of the Art Volume*, *Proc. of the Workshop on Strategies for Design and Construction of Structures to Mitigate Damage due to Cyclones*, Wind Engineering Laboratory, S.E.R.C. Madras, 75-105.

Vickery, B.J. (1995), "The response of chimneys and tower-like structures to wind loading", *State of the Art Volume, 9th Int. Conf. on Wind Engineering*, New Dehli, 205-233.

Waldeck, J.L. (1992), "The measured and predicted response of a 300m concrete chimney", *J. Wind Eng. Ind. Aerod.,* **41**, 229-240.

CC